IEEE Access
Multidisciplinary | Rapid Review | Open Access Journal

Received June 24, 2019, accepted July 14, 2019, date of publication July 22, 2019, date of current version August 8, 2019.

Digital Object Identifier 10.1109/ACCESS.2019.2930248

Flexible and Economic Dispatching of AC/DC Distribution Networks Considering Uncertainty of Wind Power

SHAN GAO[1,2], (Member, IEEE), SAI LIU[1,3], YU LIU[1,2], (Member, IEEE), XIN ZHAO[1], AND TIANCHENG E. SONG[1]

[1]School of Electrical Engineering, Southeast University, Nanjing 210096, China
[2]Jiangsu Provincial Key Laboratory of Smart Grid Technology and Equipment, Nanjing 210096, China
[3]State Grid Jiangsu Electric Power Company Ltd., Maintenance Branch Company, Nanjing 211102, China

Corresponding author: Yu Liu (yuliu@seu.edu.cn)

This work was supported in part by the Fundamental Research Funds for the Central Universities in China under Grant 2242019k30029.

ABSTRACT In order to cope with the uncertainty power and consumption problems in AC/DC distribution networks after accessing high-permeability renewable energy source (RES), a flexible economic dispatching method for the AC/DC distribution networks considering the uncertainty of wind power is proposed based on the flexibility operation theory. First, considering the flexibility of regulation range, speed, and time, the source-network-load flexibility resources of AC/DC distribution networks are quantitatively evaluated. An evaluation index and a calculation method of the operation flexibility for the AC/DC distribution networks are defined. Then, based on the nonparametric kernel density estimation and confidence interval method, the constraints transformation of flexibility requirement in distribution networks considering the uncertainty of wind power is implemented. Finally, a multi-objective day-ahead flexible and economic dispatching model of the AC/DC distribution networks is established, which takes the operation economy and voltage quality of distribution networks as the objective function and the controllable operation parameters of voltage-source converters (VSCs) and AC/DC networks as the decision variables. The modified IEEE-33 system with flexible multi-terminal interconnection is simulated and analyzed. The result shows that the proposed method further improves the node voltage level and the RES consumption level and reduces the network losses and the total dispatching cost while ensuring the AC/DC distribution network to cope with the fluctuation of the system uncertainty.

INDEX TERMS AC/DC distribution network, flexibility, uncertainty, hierarchical and partitioned strategy, economic dispatching.

I. INTRODUCTION

The deteriorating environment and the shortage of traditional energy further promote the development of renewable energy generation technology. The future distribution network will meet the requirements of access and absorption of high-permeability distributed renewable energy. China has put forward the goal of achieving 60% renewable energy source (RES) generation ratio by 2050. Europe and the United States propose to realize the power system blueprint accessing 80% and 100% RES by 2050. The power system with high proportion of RES generation has become the common goal of industrial development [1], [2]. However, the access of high-permeability RES requires higher flexibility of the system. As the development trend of distribution networks in the future, the AC/DC distribution network is an important technical method to solve the wide access and absorption of high-permeability distributed power supply in distribution networks [3]–[6]. The optimal dispatching strategy of AC/DC distribution network [7], [8] is an important technique for active control of multi-type distributed resources and voltage source converters (VSCs) to ensure the secure and economic operation of the system. However, the volatility, randomness and the uncertainty of the output of RES, the coupling of energy storage devices in time and space, and the flexibility and controllability of the operation parameters of

The associate editor coordinating the review of this manuscript and approving it for publication was Shantha Jayasinghe.

VSCs further complicate the optimal operation and scheduling of AC/DC distribution networks. The traditional optimal scheduling strategies and models of distribution networks are no longer applicable to the optimal operation of AC/DC distribution networks.

The access and absorptive capacity of intermittent and high-permeability RES generation in AC/DC distribution network and the optimal dispatching considering system flexibility have become the focus of attention and research by scholars at home and abroad. NERC defines power system flexibility as the ability to respond to the uncertainty on both sides of power supply and demand. Flexibility is the ability to dispatch existing resources to meet changes of load demands [9], [10]. According to IEA, power system flexibility means that the system responds rapidly to the large fluctuation of the load under the boundary of operation constraints. The power system makes rapid adjustments to various changes and emergencies in order to achieve the balance between supply and load [11]. Reference [12] presents a general mathematical model and a measurement index for the supply-demand balance of a multi-time scale flexibility. It also establishes a flexible expectation based on probability model. Reference [13] synthetically considers the flexible supply-demand balance and network-source coordination and establishes supply-demand flexibility index and operation flexibility index of power system respectively. It evaluates the endurance capacity of power system to uncertain factors in detail. Reference [14] establishes an optimal dispatching model for AC/DC microgrid considering high-permeability RES and electric vehicles. A three-level hierarchy consisting of DC grids, VSCs and AC grids is established with the analytical target cascading approach [15]. A decentralized optimal operation approach of AC/DC hybrid distribution networks is proposed. Reference [16] realize the optimal operation of distribution networks considering the distributed generation (DG) regulation, the switching of reactive power device, the charging and discharging control of energy storage devices, the reactive power regulation of VSCs and the reconfiguration of distribution networks. A multi-period day optimal dispatching model of AC/DC distribution networks based on second-order cone programming is constructed. A multi-scene technology based on the Markov chain is adopted to simulate the fluctuation and intermittence of wind power, photovoltaic and load in AC/DC active distribution networks [17]. A multi-time scale coordinated optimal dispatching model is proposed to control the output of tie-line and the power of flexible devices, which can better deal with the uncertainty of RES. Reference [18] considers the characteristics of time, space and direction of volatile power supply and proposes a flexibility evaluation index from the perspective of operation scheduling applied to the optimal operation of power system and the optimal dispatch of flexibility resources. An evaluation index for the flexible operation of distribution network is suggested from the perspective of flexible supply-demand balance in the context of distribution network with high-permeability of DG [19]. The optimal dispatching model meeting the flexibility constraints is established to improve flexibility when taking into account the energy storage devices and the interruptible load.

In summary, although the flexibility of power system is discussed and researched widely, there are still few methods to characterize, calculate and evaluate the flexibility for the operation of AC/DC distribution networks. Besides, the research of operation dispatching for AC/DC distribution networks considering the accurate operation losses, operation characteristics and voltage control methods of flexible DC devices as well as controllable elements is not perfect. Therefore, considering the flexibility of regulation range, speed, and time, the flexibility resources from source, network and load of AC/DC distribution networks are quantitatively evaluated for steady-state operation. The evaluation index of operation flexibility and the computing method are proposed. Secondly, the constraint transformation of the flexibility demand in distribution networks considering the uncertainty of wind power is implemented by the non-parametric kernel density estimation and confidence interval method. Then, the implementation scheme of hierarchical and partitioned dispatching strategy in AC/DC distribution networks is investigated. Considering the coordinated operation scheduling method of VSCs and controllable devices in AC/DC distribution networks, the multi-objective flexible operation dispatching method considering the uncertainty of wind power is proposed finally. The modified IEEE-33 case with multi-terminal VSC interconnections is simulated and analyzed to verify the rationality and validity of the model.

II. OPERATION FLEXIBILITY INDEX FOR AC/DC DISTRIBUTION NETWORKS WITH HIGH-PERMEABILITY RES

A. FLEXIBILITY DEMAND OF AC/DC DISTRIBUTION NETWORKS

As a platform to absorb the intermittent and distributed RES and adjust the grid structure as well as load, the flexibility demand of AC/DC distribution networks mainly comes from the uncertainty of the source, network and load sides of distribution networks, which is shown in Fig. 1. It is required that the system has sufficient flexibility regulation ability which can respond to random fluctuations of RES output and load in a certain amount of time and meet the requirements of flexible supply-demand balance.

B. FLEXIBILITY RESOURCE OF AC/DC DISTRIBUTION NETWORKS

The flexible resource of AC/DC distribution networks is characterized by rapidity, shiftability, timeliness and economy [20].The schedulable flexibility resource in AC/DC distribution networks accessing high-permeability RES exists in various forms on the power supply side, grid side and load side.

The flexibility resource on the power side includes: substations connected to the upper main network, various forms

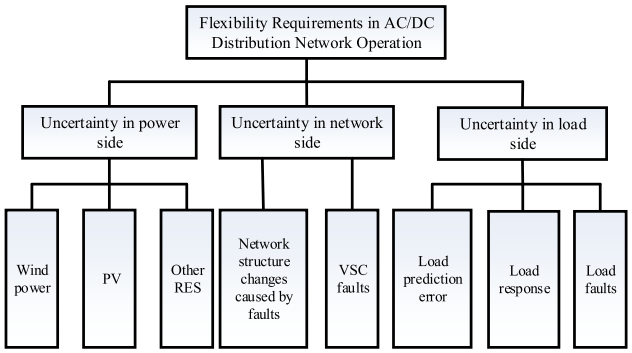

FIGURE 1. Flexibility requirements of AC/DC distribution network operation.

of distributed power generation devices, different types of energy storage devices and even wind turbine generators and photovoltaics. DG is the main source to ensure flexibility supply side. The energy storage devices are effective to further improve power quality and stabilize load fluctuations.

The flexibility resource on the grid side includes: the traditional AC distribution grid structure does not directly increase the flexibility of the system, but it can provide a secure and stable transmission channel for flexible resource dispatching. However, the AC/DC network interconnection based on the VSCs provides a channel for interconnecting the AC networks and the DC networks. The active power and reactive power injected or absorbed by nodes can be adjusted to improve the operation flexibility through the active and reactive decoupling control.

The flexible resource on the load side includes various response resources on the demand side. The response resources are various and widely distributed which can adjust the flexibility demand from the load side to improve the system flexibility.

C. CALCULATION METHOD OF OPERATION FLEXIBILITY INDEX OF AC/DC DISTRIBUTION NETWORKS

The supply-demand balance constraint of operation flexibility in distribution networks can be understood as the requirement and capability that the adequacy of various flexibility resources can meet the flexibility demand at a certain time, at a specific time scale and in a specific direction as shown below.

$$X_{\mathrm{A}}(t, \Delta t) - Y_{\mathrm{A}}(t, \Delta t) \geq \varepsilon_{\mathrm{A}} \tag{1}$$

where $X_{\mathrm{A}}(t, \Delta t)$ is the system flexibility support at time t and at a time scale Δt. $Y_{\mathrm{A}}(t, \Delta t)$ is the system flexibility demand at time t and at a time scale Δt. ε_{A} is a certain flexibility margin. $\mathrm{A} \in \{+, -\}$ expresses the direction of flexibility.

The flexible resource dispatching of AC/DC distribution networks is to improve the overall flexibility of the system based on the interaction and coordination of source-network-load flexibility resources. The following contents describes various flexibility resources, their constraints and calculation methods of AC/DC distribution networks.

1) TIME SCALE

The response characteristics of flexible resources are closely related to time scales. The determination of the corresponding time scale for system operation is the prerequisite for calculating the flexibility index. Considering the short duration of the uncertainty in the operation of AC/DC distribution networks, a large time scale should not be selected. Generally,

$$\Delta t = \{1\ \mathrm{min}, 5\ \mathrm{mins}, 15\ \mathrm{mins}, 30\ \mathrm{mins}\} \tag{2}$$

2) TRANSFORMER

The transformer flexibility refers to its capacity which can be divided into upward capacity flexibility margin and downward capacity flexibility margin. It corresponds to the upward and downward flexibility of transformers when the power fluctuates. It provides the upward or downward power support for the system. The calculation method of the transformer flexibility is as follows:

$$\begin{cases} P^t_{\mathrm{TR},i+} = P_{\mathrm{TRmax},i} - P^t_{\mathrm{TR},i} \\ P^t_{\mathrm{TR},i-} = P^t_{\mathrm{TR},i} - P_{\mathrm{TRmin},i} \\ P_{\mathrm{TRmin},i} \leq P^t_{\mathrm{TR},i} \leq P_{\mathrm{TRmax},i} \end{cases} \tag{3}$$

where $P^t_{\mathrm{TR},i+}$ and $P^t_{\mathrm{TR},i-}$ are respectively the upward capacity flexibility margin and downward capacity flexibility margin of the transformer i in the upper substation at time t. $P_{\mathrm{TRmax},i}$ and $P_{\mathrm{TRmin},i}$ are respectively the maximum and minimum allowable transmission capacity of the transformer i. $P^t_{\mathrm{TR},i}$ is the transmission power of the transformer i at time t.

3) DISPATCHABLE DG

The selection of time scales directly affects the active power output range of dispatchable DGs in distribution networks. Considering the time scale, the climbing rate and the output constraints, the calculation method of its operational flexibility is as follows:

$$\begin{cases} P^t_{\mathrm{DG},i+} = \min\left\{P_{\mathrm{DGmax},i}, P^t_{\mathrm{DG},i} + r_{\mathrm{u}} \cdot \Delta t\right\} - P^t_{\mathrm{DG},i} \\ P^t_{\mathrm{DG},i-} = \max\left\{P_{\mathrm{DGmin},i}, P^t_{\mathrm{DG},i} - r_{\mathrm{d}} \cdot \Delta t\right\} - P^t_{\mathrm{DG},i} \\ \max\left\{P_{\mathrm{DGmin},i}, P^t_{\mathrm{DG},i} - r_{\mathrm{d,i}} \cdot \Delta t\right\} \leq P^t_{\mathrm{DG},i} \\ \leq \min\left\{P_{\mathrm{DGmax},i}, P^t_{\mathrm{DG},i} + r_{\mathrm{u,i}} \cdot \Delta t\right\} \end{cases} \tag{4}$$

where $P^t_{\mathrm{DG},i}$ is the active power of DG i at time t. $P_{\mathrm{DGmax},i}$ and $P_{\mathrm{DGmin},i}$ are respectively the maximum and minimum active power of DG i. $r_{\mathrm{u},i}$, $r_{\mathrm{d},i}$ are respectively the maximum upward and downward climbing rates of DG i.

4) ENERGY STORAGE SYSTEM

The energy storage system in distribution networks can smooth the power fluctuation of RES, realize peak shaving, improve power quality and improve power regulation capability of the system. The output of energy storage devices is mainly limited by the maximum and minimum storage capacity as well as the maximum output. The calculation

method of its operational flexibility is as follows:

$$\begin{cases} P^t_{\mathrm{ESS},i+} = \min\left(P^{\mathrm{dischmax}}_{\mathrm{ESS},i}, \frac{\eta_{\mathrm{disch},i}\left(E^t_{\mathrm{ESS},i} - E_{\mathrm{ESSmin},i}\right)}{\Delta t}\right) - P^t_{\mathrm{ESS},i} \\ P^t_{\mathrm{ESS},i-} = \max\left(P^{\mathrm{chmax}}_{\mathrm{ESS},i}, \frac{\left(E_{\mathrm{ESSmax},i} - E^t_{\mathrm{ESS},i}\right)}{\eta_{\mathrm{ch},i}\Delta t}\right) - P^t_{\mathrm{ESS},i} \\ \max\left(P^{\mathrm{chmax}}_{\mathrm{ESS},i}, \frac{\left(E_{\mathrm{ESSmax},i} - E^t_{\mathrm{ESS},i}\right)}{\eta_{\mathrm{ch},i}}\Delta t\right) \le P^t_{\mathrm{ESS},i} \\ \le \min\left(P^{\mathrm{dischmax}}_{\mathrm{ESS},i}, \frac{\eta_{\mathrm{disch},i}\left(E^t_{\mathrm{ESS},i} - E_{\mathrm{ESSmin},i}\right)}{\Delta t}\right) \\ E_{\mathrm{ESSmin},i} \le E^t_{\mathrm{ESS},i} - P^t_{\mathrm{ESS},i} \cdot \Delta t \le E_{\mathrm{ESSmax},i} \\ E^t_{\mathrm{ESS},i}\Big|_{t=0} = E^t_{\mathrm{ESS},i}\Big|_{t=\mathrm{T}} \end{cases} \tag{5}$$

where $P^t_{\mathrm{ESS},i+}$, $P^t_{\mathrm{ESS},i-}$ and $P^t_{\mathrm{ESS,i}}$ are respectively the upward and downward flexibility as well as the current active power of energy storage device i at time t. The positive value represents discharging and the negative one represents charging. $E_{\mathrm{ESSmax},i}$, $E_{\mathrm{ESSmin},i}$ and $E^t_{\mathrm{ESS},i}$ are respectively the maximum and minimum storage capacity and current storage energy of energy storage device i. $\eta_{ch,i}$ and $\eta_{\mathrm{disch},i}$ are respectively the charging and discharging efficiency of energy storage device i. The fifth formula guarantees that the initial and final state of charge is same in each cycle so as to prevent the interference among dispatching cycles.

5) FLEXIBLE LOAD

The Flexible load mainly uses the following ways to increase the flexibility of the system:

- Reducing the growth rate and decline rate during peak load period.
- Reducing the peak load and increase the valley load.
- Transferring the peak load demand to the valley load period by translating load.

In this paper, the adjustable load model is adopted. The calculation method of its operational flexibility is as follows:

$$\begin{cases} P^t_{\mathrm{FL},i+} = P_{\mathrm{FLmax}} - P^t_{\mathrm{FL},i} \\ P^t_{\mathrm{FL},i-} = P_{\mathrm{FLmin}} - P^t_{\mathrm{FL},i} \\ P_{\mathrm{FLmin}} \le P^t_{\mathrm{FL},i} \le P_{\mathrm{FLmax}} \end{cases} \tag{6}$$

where $P^t_{\mathrm{FL},i+}$, $P^t_{\mathrm{FL},i-}$ and $P^t_{\mathrm{FL},i}$ are respectively the upward flexibility, the downward and the reduction quantity of flexible load i at time t. P_{FLmax} and P_{FLmin} are respectively the maximum and minimum reduction quantity of flexible load i. The compensation cost of load reduction $C\left(P^t_{\mathrm{FL},i}\right)$ should be taken into account in the economic dispatching.

6) ELECTRIC VEHICLES

The cluster charging pile of electric vehicles has a certain range of power regulation. The flexibility calculation method is as follows:

$$\begin{cases} P^t_{\mathrm{EV},i+} = P_{\mathrm{EVmax}} - P^t_{\mathrm{EV},i} \\ P^t_{\mathrm{EV},i-} = P_{\mathrm{EVmin}} - P^t_{\mathrm{EV},i} \\ P_{\mathrm{EVmin}} \le P^t_{\mathrm{EV},i} \le P_{\mathrm{EV\,max}} \end{cases} \tag{7}$$

where $P^t_{\mathrm{EV},i+}$, $P^t_{\mathrm{EV},i-}$ and $P^t_{\mathrm{EV},i}$ are respectively the upward, the downward flexibility and the reduction quantity of EV load i at time t. P_{EVmax} and P_{EVmin} are respectively the maximum and minimum reduction quantity of EV load i.

7) VOLTAGE SOURCE CONVERTERS

Compared with pure AC interconnection, AC grids interconnecting with flexible DC grids based on VSCs can decouple active power and reactive power. By adjusting the exchange power between DC and AC grids, the operation flexibility can be improved. The complementary characteristics of RES can be fully utilized in a larger space-time range to achieve a wider range of decentralized access and the fluctuation stabilization. The voltage limit and voltage fluctuation can also be improved, thereby the absorption of RES can be further improved.

The effect of VSCs on the operation flexibility of distribution networks is attributed to its active and reactive power decoupling regulation ability, whose constraints are as follows:

$$\begin{cases} U_{\mathrm{cmin},i} \le U^t_{ci} \le U_{\mathrm{cmax},i} \\ -I_{\mathrm{cmax},i} \le I^t_{ci} \le I_{\mathrm{cmax},i} \\ \left(P^t_{VSC,i}\right)^2 + \left(Q^t_{\mathrm{VSC},i}\right)^2 \le S_{\mathrm{VSC},i\mathrm{max}} \end{cases} \tag{8}$$

where $U_{\mathrm{cmax},i}$ and $U_{\mathrm{cmin},i}$ are respectively the maximum and minimum AC port voltages generated by VSC i. $I_{\mathrm{cmax},i}$ is the maximum bearable current of VSC i. U^t_{ci} and I^t_{ci} are respectively the AC port voltage and current of VSC i at time t. $P^t_{\mathrm{VSC},i}$ and $Q^t_{\mathrm{VSC},i}$ are respectively the active and reactive power transmitting to the AC side of the PCC node by VSC i at time t. $S_{\mathrm{VSC},i\mathrm{max}}$ is the maximum transmission capability of VSC i.

To sum up, the paper defines the Operation Flexibility (OF) index of AC/DC hybrid distribution networks as the active power flexibility $\left[OF^t_+, OF^t_-, \Delta t\right]$ that the system can provide in the time Δt under a certain operating state. It includes the upward operation flexibility OF^t_+ and downward operation flexibility OF^t_-. The calculation formula is as follows:

$$\begin{cases} OF^t_+ = \sum_{i=1}^{N_1} \min\left\{r_{i+}\Delta t, P_{i\,\max} - P^t_i\right\} + \sum_{i=1}^{N_2}\left(P_{i\,\max} - P^t_i\right) \\ OF^t_- = \sum_{i=1}^{N_1} \max\left\{r_{i-}\Delta t, P_{i\,\min} - P^t_i\right\} + \sum_{i=1}^{N_2}\left(P_{i\,\min} - P^t_i\right) \end{cases} \tag{9}$$

where N_1 is the total number of flexible power supplies set with climbing rate. N_2 is the total number of instantaneous flexible power supplies set. r_{i+} and r_{i-} are respectively the upward and downward ramp rate of flexible power i. Δt is

the setting time scale. $P_{i\max}$, $P_{i\min}$ and P_i^t are respectively the maximum, the minimum and the current active power of flexible power i.

III. FLEXIBILITY DEMAND MODEL OF DISTRIBUTION NETWORKS CONSIDERING UNCERTAINTY OF WIND POWER

Wind turbines are widely used in distribution networks. The uncertainty of the wind power has adverse effect on the flexible operation. In the paper, the non-parametric kernel density estimation method is used to solve the conditional probability distribution of the prediction error of wind power output under a predicted value. Based on the specific kernel function, the method which solves the error confidence interval is deduced. The flexibility constraints affected by the uncertainty of wind power in the day-ahead dispatching of AC/DC distribution networks are transformed into the deterministic constraints of operation flexibility.

A. WIND POWER PREDICTION ERROR MODEL BASED ON NON-PARAMETRIC CONDITIONAL PROBABILITY MODEL

The fitting of wind power historical sample data can be divided into two categories: parametric method and non-parametric method. Because the non-parametric estimation method does not need to assume the probability distribution form beforehand. It only needs to study the distribution characteristics from the actual historical data and has high fitting accuracy. In the paper, the non-parametric kernel density estimation method is used to fit the probability distribution of wind power prediction errors. In addition, considering the power correspondence among prediction errors, the actual values and the predicted values of wind power, the fluctuation range of wind power prediction errors is different when the predicted value is different. It is obviously unreasonable to directly fit and analyze the prediction errors under all the power values. Therefore, the conditional probability model of wind power prediction errors can be constructed to calculate the probability distribution of wind power prediction errors under a predicted value. The reasonableness and accuracy of the confidence interval solution for wind power prediction errors can be improved.

The absolute error of wind power output at time t is:

$$e_t = P'_{\mathrm{W}t} - P_{\mathrm{W}t} \tag{10}$$

where P'_{Wt} and P_{Wt} are respectively the prediction and actual value.

The error distribution of a predicted value is represented based on the conditional probability model and its probability density function is $f\left(e\left|P'_{\mathrm{W}t}\right.\right)$. The normalization of e_t is carried out by taking the wind farm rated installed capacity P_{Wc} as the reference value. The purpose is to make the range of predicted and actual values in $[0, 1]$ and the range of absolute errors in $[-1, 1]$.

$$e = \frac{e_t}{P_{\mathrm{Wc}}} \tag{11}$$

Because the overall prediction errors possess the non-uniformity related to the value of itself, the probability distribution of the errors can be solved after segmentation according to the predicted power value. The wind power outputs are divided into n intervals. When $n = 10$, The corresponding interval length is 0.1p.u., $i = 1, 2, \cdots, n$. The ith prediction power interval is noted as $P'_{\mathrm{W}i}$. The conditional probability density function of prediction errors in the ith prediction power interval is $f\left(e\left|P'_{\mathrm{W}i}\right.\right)$. The cumulative probability distribution of the i th prediction power interval is $F\left(e\left|P'_{\mathrm{W}i}\right.\right)$. They can be noted $f(e)$ and $F(e)$ simply.

$e_{i1}, e_{i2}, \cdots, e_{in}$ is a set of random samples extracting from the ith output interval attaching to the total sample of wind power prediction errors E.

The unknown probability density of the set of samples is assumed as $f_i(e)$. $\hat{f}_i(e)$ represents its kernel density estimate as follows:

$$\hat{f}_i(e) = \frac{1}{nh}\sum_{j=1}^{n} K\left(\frac{e - e_{ij}}{h}\right) \tag{12}$$

where n is the total number of the sample data for the ith interval. h is the window width which is the smoothing parameter. e_{ij} is the sample data. $K(\cdot)$ is the kernel function. $\hat{f}_i(e)$ is related to the total sample size, h and $K(\cdot)$.

B. CONFIDENCE INTERVAL ESTIMATION OF WIND POWER PREDICTION ERRORS APPLIED TO FLEXIBLE DAY-AHEAD DISPATCHING

The confidence interval of wind power prediction errors is derived by using the Gauss kernel function. The Gauss kernel function and its kernel density estimation formula are as follows:

$$\begin{cases} K(e) = \dfrac{1}{\sqrt{2\pi}}\exp\left[-\dfrac{1}{2}\left(\dfrac{e - e_{ij}}{h}\right)^2\right] \\ \hat{f}_i(e) = \dfrac{1}{\sqrt{2\pi}nh}\displaystyle\sum_{j=1}^{n}\exp\left[-\frac{1}{2}\left(\frac{e - e_{ij}}{h}\right)^2\right] \end{cases} \tag{13}$$

Based on the probability theory, the cumulative probability distribution of prediction errors in the interval $[a, b]$ is as follows:

$$\begin{aligned} F_i(a \le e \le b) &= \int_a^b \hat{f}_i(e)\mathrm{d}e \\ &= \frac{1}{\sqrt{2\pi}nh}\int_a^b \sum_{j=1}^{n}\exp\left[-\frac{1}{2}\left(\frac{e - e_{ij}}{h}\right)^2\right]\mathrm{d}e \end{aligned} \tag{14}$$

The integral part of the above equation is difficult to be solved by the specific analytical formula, but its numerical solution can be obtained by numerical analysis. The integral

part can be noted as I. The upper formula is:

$$\begin{cases} I = \int_a^b \hat{f}_i^*(e)\mathrm{d}e \\ \hat{f}_i^*(e)\mathrm{d}e = \sum_{j=1}^{n} \exp\left[-\frac{1}{2}\left(\frac{e-e_{ij}}{h}\right)^2\right] \end{cases} \tag{15}$$

The formula can be solved by Gauss quadrature formula. Make $e = \frac{b-a}{2}t + \frac{a+b}{2}$, thus

$$\begin{aligned} I &= \int_a^b \hat{f}_i^*(e)\mathrm{d}e = \frac{b-a}{2}\int_{-1}^{1} \hat{f}_i^*\left(\frac{b-a}{2}t + \frac{a+b}{2}\right)\mathrm{d}t \\ &= \frac{b-a}{2}\int_{-1}^{1} \hat{f}_i^{**}(t)\mathrm{d}t \end{aligned} \tag{16}$$

The above process realizes the transformation of the integral as shown below.

$$\begin{cases} I = \frac{b-a}{2} I^* \\ I^* = \frac{b-a}{2}\int_{-1}^{1} \hat{f}_i^{**}(t)\,dt \\ \hat{f}_i^{**}(t) = \hat{f}_i^*\left(\frac{b-a}{2}t + \frac{a+b}{2}\right) \end{cases} \tag{17}$$

The application condition of Gauss quadrature formula is satisfied in the above formula I^*. The solution formula is as follows:

$$I^* = \frac{b-a}{2}\int_{-1}^{1} \hat{f}_i^{**}(t)\,dt = \frac{b-a}{2}\sum_{k=0}^{m} \tilde{A}_k \hat{f}_i^{**}(t_k) \tag{18}$$

t_k is the quadrature node for Gauss. $\tilde{A}_k$ is the corresponding quadrature coefficient. Taking the five-point Gauss quadrature formula as an example, the following formula can be gotten:

$$\begin{aligned} I^* &= \frac{b-a}{2} \\ &\times \begin{Bmatrix} 0.569\hat{f}_i^{**}(0) + 0.479\left[\hat{f}_i^{**}(0.538) + \hat{f}_i^{**}(-0.538)\right] \\ + \ldots\ldots + 0.237\left[\hat{f}_i^{**}(0.906) + \hat{f}_i^{**}(-0.906)\right] \end{Bmatrix} \end{aligned} \tag{19}$$

Through the above deduction process, the probability distribution function of prediction errors of wind power outputs in the interval $[a, b]$ is as follows:

$$F_i(a \le e \le b) = F_i(-1 \le t \le 1) = \frac{1}{\sqrt{2\pi}nh} I^* \tag{20}$$

Assuming that predicted outputs of wind power is P'_{Wi}, its original probability density function is $f_i(e)$. The corresponding kernel density estimation is $\hat{f}_i(e)$ and its corresponding probability distribution function is $F_i(e)$. Given $\alpha(0 < \alpha < 1)$, the confidence interval of prediction error under the confidence $1-\alpha$ is expressed as $[e_{\mathrm{Wi,lower}}, e_{\mathrm{Wi,upper}}]$ when the wind power output is P'_{Wi}. $e_{\mathrm{Wi,lower}}$ and $e_{\mathrm{Wi,upper}}$ are respectively the lower and upper bounds of the confidence interval.

$$F_i\left(e_{\mathrm{Wi,lower}} < e < e_{\mathrm{Wi,upper}}\right) = 1-\alpha \tag{21}$$

Because $-1 \le t \le 1$, the following formula can be gotten according to the quantile theory.

$$\begin{cases} F_i\left(-1 \le t \le e_{\mathrm{Wi,lower}}\right) = \frac{\alpha}{2} \\ F_i\left(-1 \le t \le e_{\mathrm{Wi,upper}}\right) = 1 - \frac{\alpha}{2} \end{cases} \tag{22}$$

Thus, the upper and lower bounds of the confidence interval of prediction errors through the inverse cumulative probability distribution are respectively:

$$\begin{cases} e_{\mathrm{Wi,lower}} = F_i^{-1}\left(\frac{\alpha}{2}\right) \\ e_{\mathrm{Wi,upper}} = F_i^{-1}\left(1-\frac{\alpha}{2}\right) \end{cases} \tag{23}$$

Through the above deduction process, the uncertain influence of wind power on the flexibility demand of distribution networks $\left[OF_+^t, OF_-^t, \Delta t\right]$ is transformed into the deterministic constraint. The flexibility constraint (1) of AC/DC distribution networks operation can be converted into the following formula. Based on the formula, the flexible demand transformation and characterization of the uncertainty of wind power in the economic dispatching can be realized when the dispatching result satisfies both economic and flexible requirements.

$$\begin{cases} OF_+^t - \varepsilon_+ \ge e_{\mathrm{Wi,upper}} = F_i^{-1}\left(1-\frac{\alpha}{2}\right) \\ OF_-^t - \varepsilon_- \le e_{\mathrm{Wi,lower}} = F_i^{-1}\left(\frac{\alpha}{2}\right) \end{cases} \tag{24}$$

IV. FLEXIBLE AND ECONOMIC DISPATCHING OF AC/DC DISTRIBUTION NETWORKS

The flexible and economic dispatching model of AC/DC distribution networks adopts the hierarchical and partitional dispatching strategy. Considering the flexibility requirement of the distribution networks operation, the quantitative flexibility index constraints are incorporated into the dispatching model to ensure that the economic dispatching scheme can maximize economic benefits and meet the flexible adjustment requirement of AC/DC distribution networks accessing high-permeability RES.

A. HIERARCHICAL AND PARTITIONAL DISPATCHING STRATEGY

In the paper, the dispatching of AC/DC distribution networks is divided into the local dispatching layer, the power flow control layer and the regional dispatching layer in turn, as shown in Fig. 2.

The RES outputs in local dispatching layer are random, volatile and uncertain, so RES is bundled with an energy storage device as an optimization subject. In this paper, a wind turbine generator and an energy storage device are combined as a subject and its decision variable is the output of the energy storage device P_{ESS}^t. After completing the optimization goal of the local dispatching layer, the results are reported

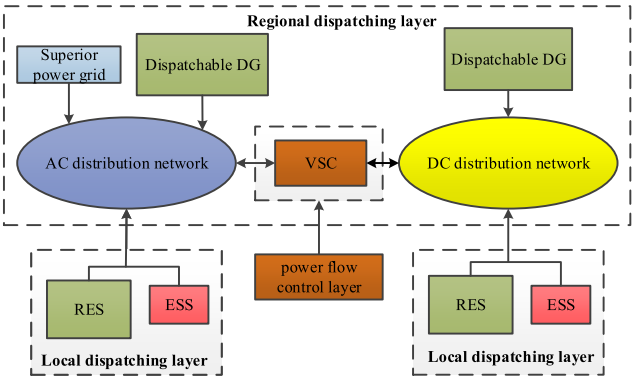

FIGURE 2. Schematic diagram of hierarchical and partitioned optimal dispatching for AC/DC distribution networks.

to the regional dispatching layer. The optimization objectives of the local scheduling layer are defined as Obj1: Adjusting the peak-valley difference of the combined output, Obj2: Reducing the fluctuation of the wind power output, Obj3: The combined output fits the change trend of load nodes nearby. They are shown below.

$$\begin{cases} Obj1: \min \dfrac{1}{T}\displaystyle\sum_{t=1}^{T}\left(P_{\mathrm{WT}}^{t}+P_{\mathrm{ESS}}^{t}-\bar{P}_{\mathrm{WT,ESS}}\right)^{2} \\ Obj2: \min \displaystyle\sum_{t=1}^{T-1}\left|P_{\mathrm{WT,ESS}}^{t+1}-P_{\mathrm{WT,ESS}}^{t}\right| \\ Obj3: \min \dfrac{1}{\bar{P}_{L}}\sqrt{\dfrac{1}{T}\displaystyle\sum_{t=1}^{T}\left(P_{\mathrm{WT}}^{t}+P_{\mathrm{ESS}}^{t}-P_{\mathrm{L}}^{t}\right)^{2}} \\ \bar{P}_{\mathrm{WT,ESS}}=\displaystyle\sum_{t=1}^{T}\left(P_{\mathrm{WT}}^{t}+P_{\mathrm{ESS}}^{t}\right) \\ P_{\mathrm{WT,ESS}}^{t}=P_{\mathrm{WT}}^{t}+P_{\mathrm{ESS}}^{t} \end{cases} \tag{25}$$

where P_{WT}^{t} and P_{ESS}^{t} are respectively the output of wind turbines and energy storage devices at time t. $P_{\mathrm{WT,ESS}}^{t}$ and $\bar{P}_{\mathrm{WT,ESS}}$ are respectively the combined output value and mean value of wind-storages. P_{L}^{t} and $\bar{P}_{\mathrm{L}}$ are respectively the total load and the average value of main load nodes near the wind turbine at time t.

The regional dispatching layer modifies the corresponding operation parameters in the network according to the optimization results of the local dispatching layer. Then it schedules other control parameters including the electricity purchased from the upper power grid, the schedulable RES output, the controllable gas engine output, the flexible load reduction, the regulation of electric vehicles and reactive power compensation devices.

The power flow control layer adjusts control parameters of VSCs according to the specific dispatching result to further realize the optimal power flow control so that the distribution network meets the flexibility constraints and realizes the economic operation.

B. OBJECTIVE FUNCTION AND CONSTRAINTS

1) OBJECTIVE FUNCTION

The flexible economic dispatching model of AC/DC distribution networks accessing high-permeability RES is established by integrating the economic operation and the voltage quality of nodes. The model is a multi-objective optimization problem with the following objective function.

$$\begin{cases} \min F_1 = \displaystyle\sum_{t=1}^{N_t} C_{MG}^{t}+\sum_{t=1}^{N_t} C_{\mathrm{WT}}^{t}+\sum_{t=1}^{N_t} C_{\mathrm{PV}}^{t}+\sum_{t=1}^{N_t} C_{\mathrm{ESS}}^{t} \\ \qquad\quad +\displaystyle\sum_{t=1}^{N_t} C_{\mathrm{FL}}^{t}+\sum_{t=1}^{N_t} C_{\mathrm{MT}}^{t}+\sum_{t=1}^{N_t} C_{\mathrm{EV}}^{t}+\sum_{t=1}^{N_t} C_{\mathrm{WPP}}^{t} \\ \min F_2 = \displaystyle\sum_{i=1}^{N_{\mathrm{AC}}}\left(\frac{U_{\mathrm{AC},i}^{t}-U_{\exp}}{\Delta U_{\max}}\right)^{2}+\sum_{i=1}^{N_{\mathrm{DC}}}\left(\frac{U_{\mathrm{DC},i}^{t}-U_{\exp}}{\Delta U_{\max}}\right)^{2} \end{cases} \tag{26}$$

$$\begin{cases} C_{\mathrm{MG}}^{t}=c_{\mathrm{ep}}^{t}\cdot P_{\mathrm{MG}}^{t}\Delta t \\ C_{\mathrm{WT}}^{t}=c_{\mathrm{wt}}\cdot P_{\mathrm{WT}}^{t}\Delta t \\ C_{\mathrm{PV}}^{t}=c_{\mathrm{pv}}\cdot P_{\mathrm{PV}}^{t}\Delta t \\ C_{\mathrm{ESS}}^{t}=c_{\mathrm{ess}}\cdot P_{\mathrm{ESS}}^{t}\Delta t \\ C_{\mathrm{FL}}^{t}=c_{\mathrm{fl}}\cdot P_{\mathrm{fl}}^{t}\Delta t \\ C_{\mathrm{MT}}^{t}=c_{\mathrm{mt}}\cdot P_{\mathrm{MT}}^{t}\Delta t \\ C_{\mathrm{EV}}^{t}=c_{\mathrm{ev}}\cdot P_{\mathrm{EV}}^{t}\Delta t \\ C_{\mathrm{WPP}}^{t}=\left(c_{\mathrm{wp}}\cdot P_{\mathrm{WC}}^{t}+c_{\mathrm{pp}}\cdot P_{\mathrm{PC}}^{t}\right)\Delta t \end{cases} \tag{27}$$

where C_{MG}^{t} is the cost of the electricity purchased by distribution networks from the superior main network at time t. c_{ep}^{t} is the time-of-use electricity price at time t. P_{MG}^{t} is the purchasing power from the superior main network at time t. C_{WT}^{t} and C_{PV}^{t} are respectively the operation and maintenance costs of an wind turbine generator and an photovoltaic power generator at time t. c_{wt} and c_{pv} are respectively the unit operating and maintenance costs of an wind turbine generator and an photovoltaic power generator at time t. P_{WT}^{t} and P_{PV}^{t} are respectively the outputs of an wind turbine generator and an photovoltaic power generator at time t. C_{ESS}^{t} is the operation and maintenance cost of energy storage devices at time t. c_{ess} is the unit operation and maintenance cost for charging and discharging of an energy storage device. P_{ESS}^{t} is the charging and discharging power of an energy storage device at time t. C_{FL}^{t} is the compensation cost for the flexible load at time t. c_{fl} is the unit compensation cost for the flexible load. P_{fl}^{t} is the reduction of electricity for the flexible load at time t. C_{MT}^{t} is the cost of fuel, operation and maintenance for an micro gas turbine. c_{mt} is the unit generation cost of an micro gas turbine. P_{MT}^{t} is the output of an micro gas turbine at time t. C_{EV}^{t} is the operation and management cost of the adjustable load such as charging piles. c_{ev} is its operation and maintenance cost of per unit electric quantity. P_{EV}^{t} is the load of charging piles at time t. C_{WPP}^{t} is the penalty charges for the abandoned wind power and photovoltaic power at time t. c_{wp} and c_{pp} are respectively the penalty cost coefficients of unit electricity for the abandoned wind power and

photovoltaic power. P^t_{WC} and P^t_{PC} are respectively the abandoned wind power and photovoltaic power at time t. U_{AC}, i^t and U_{DC}, i^t are respectively the voltage value of AC nodes and DC nodes. U_{exp} is the node voltage expectation ($U_{\mathrm{exp}} =$ 1.0p.u. in the paper). $\Delta U_{\max}$ is the maximum allowable node voltage deviation ($\Delta U_{\max} = 0.05$p.u. in the paper.).

2) CONSTRAINTS

The equality constraints consist of the power flow balance equation of AC systems and the active power balance equation of DC systems.

$$\begin{cases} \Delta P_i = U_i \sum_{j\in i} U_j(G_{ij}\cos\theta_{ij} + B_{ij}\sin\theta_{ij}) \\ \qquad -(P_{\mathrm{DG}i} + P_{si} - P_{\mathrm{d}i}) = 0 \\ \Delta Q_i = U_i \sum_{j\in i} U_j(G_{ij}\sin\theta_{ij} - B_{ij}\cos\theta_{ij}) \\ \qquad -(Q_{\mathrm{DG}i} + Q_{si} - Q_{\mathrm{d}i}) = 0 \\ \Delta \mathrm{P_{dc}}i = \mathrm{P_{dc}}i - \sum_{j=1}^{n} Y_{ij}U_{\mathrm{dc}j}U_{\mathrm{dc}}i = 0 \end{cases} \tag{28}$$

where ΔP_i and ΔQ_i are the power deviations of the AC node i. $P_{\mathrm{DG}i}$ and $Q_{\mathrm{DG}i}$ are respectively the active and reactive outputs of DG i. P_{si} and Q_{si} are respectively the injected active and reactive power of the AC node i. $P_{\mathrm{d}i}$ and $Q_{\mathrm{d}i}$ are respectively the active and reactive power injected to the AC side of PCC node i by VSC. θ_{ij} is the phase difference between the node i and j. $G_{ij} + jB_{ij}$ is the admittance between the node i and j. $P_{\mathrm{dc}i}$ is the active power injected into the DC grid by the DC node.

The inequality constraints are composed of AC/DC system operation constraints, VSCs operation constraints, operation flexibility constraints and control variables constraints in distribution networks.

The inequality constraints that AC and DC systems need to satisfy include the upper and lower limits of node voltages, transmission power constraints and upper and lower limits of line currents.

$$\begin{cases} U_{\mathrm{aci\,min}} \le U_{\mathrm{aci}} \le U_{\mathrm{aci\,max}} \\ |P_{ij}| \le P_{ij\,\max} \\ \mathrm{U_{dc}}i_{\min} \le U_{\mathrm{dc}i} \le \mathrm{U_{dc}}i_{\max} \\ \text{-}\mathrm{I_{dc}}ij_{max} \le \mathrm{I_{dc}}ij \le \mathrm{I_{dc}}ij_{max} \end{cases} \tag{29}$$

where $U_{\mathrm{aci\,max}}$ and $U_{\mathrm{aci\,min}}$ are respectively the upper and lower limits of node voltages. $P_{ij\,\max}$ is the upper limit of the active power of the DC branch i-j. $\mathrm{U_{dc}}i_{\max}$ and $\mathrm{U_{dc}}i_{\min}$ are respectively the maximum and minimum voltages of the DC node i. $\mathrm{I_{dc}}ij_{\max}$ is the maximum current of the DC branch i-j.

The operation constraints of VSCs are shown in (8) which is represented in Fig. 3.

The constraints of operation flexibility and control variables include flexible resources constraints (3-8) and operational constraints of controllable devices in distribution networks.

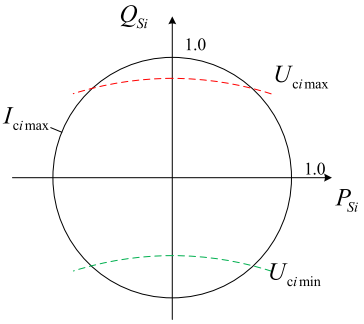

FIGURE 3. Operation range of VSCs under voltage and current constraints.

$$\begin{cases} T_{i\min} \le T_i \le T_{i\max} \\ Q_{ci\min} \le Q_{ci} \le Q_{ci\max} \\ (1-\lambda_{\mathrm{WT}})\,P_{\mathrm{WT},i\max} \le P_{\mathrm{WT},i} \le P_{\mathrm{WT},i\max} \\ (1-\lambda_{\mathrm{PV}})\,P_{\mathrm{PV},i\max} \le P_{\mathrm{PV},i} \le P_{\mathrm{PV},i\max} \\ P^2_{\mathrm{PV},i} + Q^2_{\mathrm{PV},i} \le S^2_{\mathrm{PV},i} \end{cases} \tag{30}$$

where $T_{i\max}$ and $T_{i\min}$ are respectively the upper and lower limit of transformer taps. $Q_{ci\max}$ and $Q_{ci\min}$ are respectively the upper and lower output limit of reactive power compensation devices include shunt capacitor banks and static var compensators at the node i. λ_{WT} and λ_{PV} are respectively the upper limit value of the abandoned wind power and photovoltaic power. $P_{\mathrm{WT},i\max}$ and $P_{\mathrm{PV},i\max}$ are respectively the maximum output of the wind power and photovoltaic power currently. $Q_{\mathrm{PV},i}$ is the reactive power of photovoltaic power. $S_{\mathrm{PV},i}$ is the maximum capacity of the photovoltaic device i.

C. MODEL SOLUTION

Aiming at the above multi-objective optimization problem, the linear weighted summation method is used to simplify it. The weight coefficients and normalization method are used to transform the multi-objective problem into a single-objective model shown as follows:

$$\begin{cases} \min F = \omega_1 \dfrac{F_1 - F_{1\min}}{F_{1\max} - F_{1\min}} + \omega_2 \dfrac{F_2 - F_{2\min}}{F_{2\max} - F_{2\min}} + P(R) \\ \omega_1 + \omega_2 = 1 \\ PU(R) = \begin{cases} 0 & R \ge 0 \\ 10^8 * |R| & R < 0 \end{cases} \end{cases} \tag{31}$$

where ω_1 and ω_2 are weight coefficients. The paper makes $\omega_1 = 0.75, \omega_2 = 0.25$ based on the expert experience combined with the actual situation. $PU(R)$ is a penalty function where constraints of node voltages and flexibility are introduced. $|R|$ represents the exceeding limit of constraints. $R \ge 0$ means constraints are satisfied and $R < 0$ means constraints are not satisfied.

The decision variables are divided into two categories according to voltage control modes of VSCs:

Single-point voltage control:

$$[\boldsymbol{U}_{\mathrm{dc}}\ \boldsymbol{P}_{\mathrm{s}}\ \boldsymbol{Q}_{\mathrm{s}}\ \boldsymbol{U}_{\mathrm{s}}\ \boldsymbol{M}_{\mathrm{AC-DC}}]$$

Voltage-droop control:

$$[\boldsymbol{k}_{\mathrm{p}}\ \boldsymbol{U}_{\mathrm{dcref}}\ \boldsymbol{P}_{\mathrm{dcref}}\ \boldsymbol{P}_{\mathrm{s}}\ \boldsymbol{Q}_{\mathrm{s}}\ \boldsymbol{U}_{\mathrm{s}}\ \boldsymbol{M}_{\mathrm{AC-DC}}]$$

$\boldsymbol{U}_{\mathbf{dc}}$ is the DC voltages of VSCs. $\boldsymbol{P}_{\mathbf{s}}$, $\boldsymbol{Q}_{\mathbf{s}}$ and $\boldsymbol{U}_{\mathbf{s}}$ are respectively the active power, reactive power inflowing into the AC grid through VSCs and the AC voltages of PCC nodes. $\boldsymbol{M}_{\mathbf{AC-DC}}$ is the matrix of active management element parameters in AC/DC distribution network. $\boldsymbol{k}_{\mathbf{p}}$ is the droop coefficient of VSCs. $\boldsymbol{P}_{\mathbf{dcref}}$ and $\boldsymbol{U}_{\mathbf{dcref}}$ are set values of active power and voltage for the original reference point of operation respectively.

The droop coefficients of voltage stations are mainly set in advance according to its capacity and real-time operation status, so $\boldsymbol{k}_{\mathbf{p}}$ is not frequently adjusted during the operation. In the paper, only the original active power setting values $\boldsymbol{P}_{\mathbf{dcref}}$ and the original voltage setting values $\boldsymbol{U}_{\mathbf{dcref}}$ are selected as the decision variables in the voltage-droop control mode.

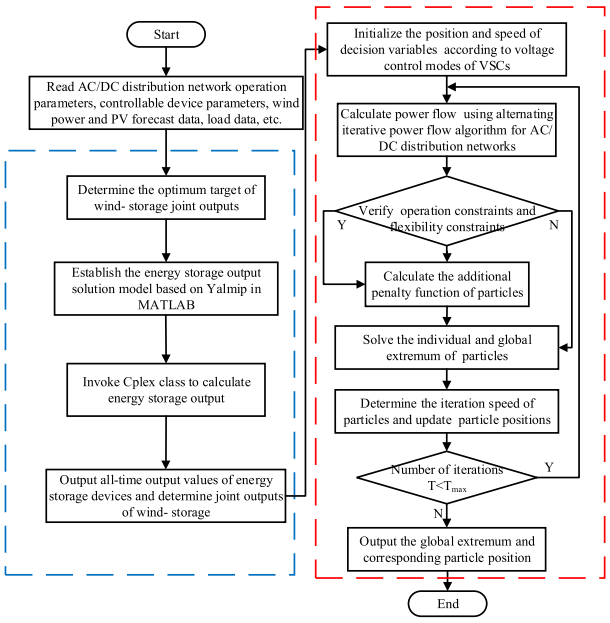

FIGURE 4. Flow chart of flexible economic dispatching for AC/DC distribution networks.

Aiming at the above single objective optimization model with non-linearity, multi variables and multi constraints, the paper uses Yalmip&Cplex, alternating iterative power flow algorithm for hybrid AC/DC networks [21] and dual particle swarm optimization algorithm to build and solve the model. Fig. 4 shows the detailed model solving step in which the blue box corresponds to the local dispatching layer and the red box corresponds to the regional dispatching layer. The following are the concrete steps to solve the flexible economic dispatching model: Obtain the network parameters of AC/DC distribution networks: the relevant operating parameters, constraints of various controllable devices, the day-ahead predictive output of wind turbines, photovoltaic generators and electric vehicles; Aiming at the local dispatching layer, according to the optimization objective, the combined output of wind-storage is optimized by using Yalmip&Cplex, and full-time charging and discharging powers of energy storages are determined under the condition of meeting the output constraints and capacity constraints; Aiming at the regional dispatching layer, after obtaining the operation mode of the local dispatching layer, the control parameters of controllable devices and VSCs are optimized based on alternating iterative power flow algorithm for hybrid AC/DC networks and dual particle swarm optimization algorithm. Under the condition of satisfying the operation constraints and flexibility constraints, the flexible economic dispatching scheme of AC/DC distribution networks is determined with the goal of optimizing the economy and voltage quality.

V. CASE ANALYSIS

A. CASE DESCRIPTION

At present, the widely used probability models for wind power prediction errors include the normal distribution [22], t-location-scale distribution [23] and Beta distribution [24]. Because Beat distribution is defined in [0,1], it only can fit errors in one direction. In order to verify the advantages of the non-parametric kernel density estimation method, the paper compare it with the fitting results of the normal distribution and t-location-scale distribution. The predicted and actual wind power outputs of the small wind farm in a distribution network in winter are taken as the studying case. The time resolution of data acquisition is 15 minutes.

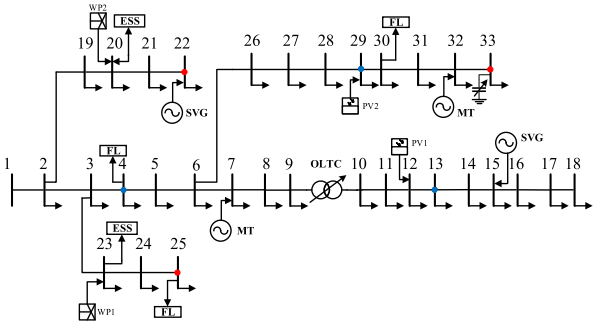

FIGURE 5. Modified topology of IEEE-33 system.

The proposed flexible economic dispatching model for AC/DC distribution networks is modeled and analyzed by the modified IEEE-33 system interconnected with the multi-terminal flexible DC grid. The topology of the modified IEEE-33 system is shown in Fig. 5 and its load parameters are shown in Appendix-Table 4. In the AC network, the branch 9-10 is connected with an on-load tap changer transformers (OLTC). The voltage regulation range is 0.95p.u.∼1.05p.u. and the adjustment step is 0.005p.u.. The shunt reactive power compensators (SCP) are connected to the node 33. The adjusting range is 0∼0.4Mvar and the adjusting step is

0.02Mvar. Static var generators (SVG) are connected to the nodes 15 and 22 with a regulation range of −0.4∼0.5Mvar and −0.3∼0.4Mvar respectively. Wind turbines (WT) and energy storage systems (ESS) are connected to the AC node 20, 23 and DC node 6 respectively. The maximum power of wind turbines is 0.5MW, 0.6MW and 0.5MW respectively. Detailed parameters of energy storage systems are shown in Appendix-Table 5.

Photovoltaic generators are connected to the AC node 12, 29 and DC node 5 and the maximum powers are 0.5MW, 0.4MW and 0.4MW respectively. Micro gas turbines are connected to the AC nodes 7 and 32 with the maximum power of 0.5MW and 0.4MW as well as climbing rates of 12kW/min and 10kW/min respectively. The AC node 25 and 30 are selected as flexible load (FL) nodes and the DC node 4 is selected as the EV vehicle load. The upper limit of load reduction is 20% real-time load. The AC distribution network is interconnected with a three-terminal MTDC network with a voltage level of ±7.5kV. The specific topology of the DC network is shown in Fig. 6.

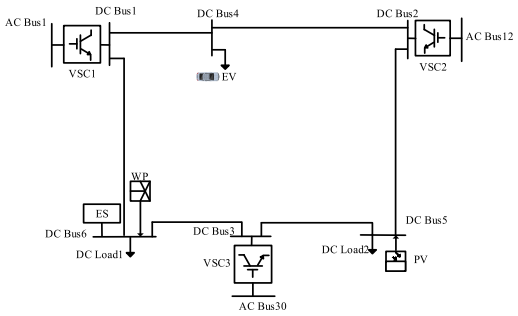

FIGURE 6. Topology of DC network.

The reference capacity of the AC/DC distribution network is 10 MVA. The reference voltage of DC network is 7.5 kV. The VSC nodes 1, 2 and 3 are connected with the AC distribution network nodes 1, 15 and 27 respectively. The DC nodes 4, 5 and 6 are pure DC nodes. The DC load parameters are shown in Appendix-Table 6. The operation parameters of VSCs and DC network parameters are shown in Appendix-Table 7 and Appendix-Table 8 respectively.

The time-of-use power price is adopted for the purchase price of power from the upper power grid shown in Appendix-Table 9. The operation and maintenance cost coefficients of various devices is shown in Appendix-Table 10. The predicted outputs and load values of wind power and photovoltaic power are shown in Fig. 7. The maximum load is 5.7465MW and the total installed capacity of wind power and photovoltaic is 2.9MW, so the RES permeability is over 50%.

B. SIMULATION RESULTS AND ANALYSIS

1) ANALYSIS OF OPERATION FLEXIBILITY DEMAND MODEL OF THE AC/DC DISTRIBUTION NETWORK

Fig. 8 illustrates the comparison of the fitting effect of the kernel density estimation method with the normal distribution

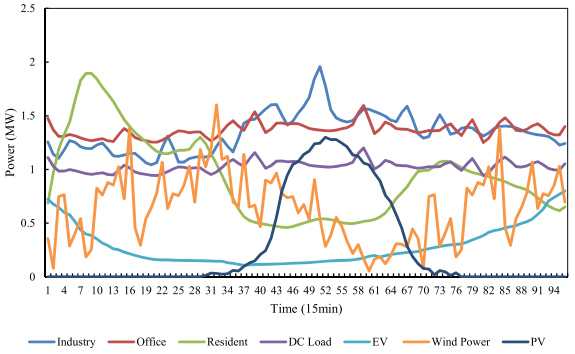

FIGURE 7. Load, wind power and photovoltaic output of the distribution network.

and t-location-scale distribution when the per-unit value of the predicted values is in the interval [0,0.1], [0.2,0.3], [0.5,0.6] and [0.9,1.0]. The wind power prediction errors in Fig. 8 are the per-unit values in [−1,1] and the vertical axis represents the probability density.

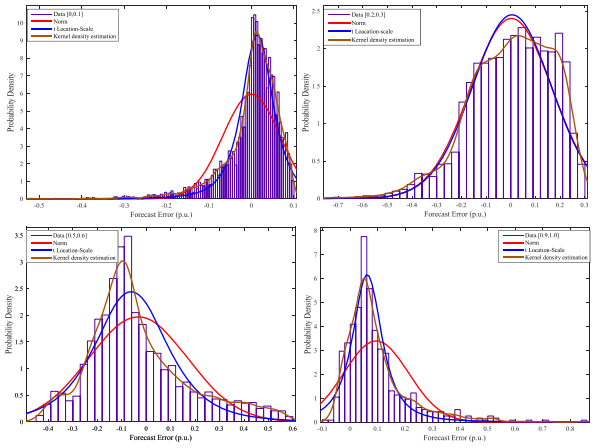

FIGURE 8. Comparison of error fitting effect in some prediction intervals.

It can be seen from Fig. 8 that:

The distribution of error data in different prediction power intervals varies greatly. The probability distributions present the characteristics of left-sided, right-sided, peak, multi-peak and trail, among which fitting of spike and multi-peak is the difficulty of error analysis.

Because the prediction error has left or right deviation attributes, and the unbiasedness of normal distribution leads to inadequate fitting of kurtosis. For peak and multi-peak, the fitting effect is obviously poor. Generally speaking, the normal distribution is the worst among the three fitting methods.

Because t-location-scale distribution has location and scale parameters, its fitting effect for multi-peak, peak and trail has been greatly improved compared with the normal distribution. However, as shown in the interval [0.5,0.6], t-location-scale distribution still has the inadequate fitting phenomenon

for peak bulge and over-estimating the concave part of the probability distribution.

Conventional parameter distribution fitting model cannot well characterize the multi-peak and peak characteristics of wind power prediction errors. Compared with the normal distribution model and t-location-scale model, the non-parametric kernel density estimation method characterizes the multi-attribute characteristics of wind power prediction errors better. As the fitting result of the interval [0.2,0.3] shows, the curve of kernel density estimation better fits the prediction error distribution. The maximum logarithmic likelihood value can be regarded as the goodness of the fit index. The maximum logarithmic likelihood values of corresponding results in the interval [0.2,0.3] are 2176, 2180.45 and 0.0339 respectively. It can be seen that the fitting effect of kernel density estimation is much better. The conditional probability model based on the kernel density estimation can be used as the error analysis method to obtain more reasonable and accurate scheduling results.

TABLE 1. Confidence intervals of some power intervals under different confidence degrees.

Confidence degree	Prediction interval		
	[0,0.1]	[0.5,0.6]	[0.9,1.0]
0.80	[-0.082,0.067]	[-0.253,0.275]	[-0.017,0.243]
0.90	[-0.129,0.080]	[-0.323,0.401]	[-0.035,0.340]
0.95	[-0.181,0.088]	[-0.372,0.479]	[-0.049,0.427]

Taking the above wind power error data as the analysis object, the confidence intervals under different prediction error intervals and different confidence degrees are calculated. Some results are listed in Table 1. It can be seen that the confidence intervals of different power intervals have great differences under the same confidence level. The confidence intervals of the same power interval have obvious differences with the change of confidence level which is closely related to the distribution shape of the original error data. The left boundary of the confidence interval in the interval [0,0.1] increases gradually and the right boundary changes slowly under the confidence levels of 0.8, 0.9 and 0.95, which is consistent with the trailing characteristics of the left side. In this paper, the flexibility requirement transformation considering the uncertainty of wind power is realized with the above case. As shown in Fig. 9, it is considered as the flexible requirement constraint for the economic dispatching model.

2) SIMULATION ANALYSIS OF THE DAY-AHEAD FLEXIBLE ECONOMIC DISPATCHING

In order to verify the effectiveness of the flexible dispatching model, the AC/DC distribution network is simulated and analyzed based on the basic parameters and the flexibility requirement constraints which take the uncertainty of wind

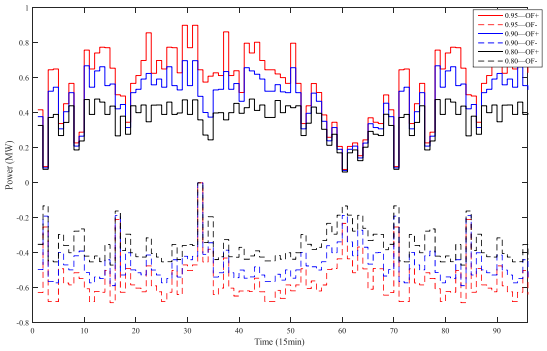

FIGURE 9. Flexibility requirement constraints for the AC/DC distribution network with different confidence degrees.

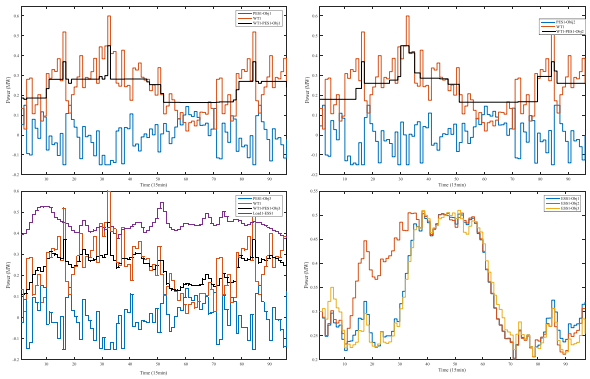

FIGURE 10. Optimization results of local dispatching layer at Node 23.

power into account. Yalmip&Cplex are used to solve the local scheduling layer and double particle swarm optimization is used to solve the regional scheduling layer. The particle swarm size is set to 150. The inertia weight is $\omega = 0.5$. Two acceleration factors are $c1 = 1$, $c2 = 2$. The iteration times are set to 150. Fig. 10 shows the optimization results of local dispatching layer at the node 23. The control objectives 1∼3 can effectively suppress wind power fluctuations, reduce the maximum and minimum output difference of the wind power. The capacity of energy storage devices at the first and last moment are basically consistent. The trend of the combined output of wind-storage at the node 23 under the control objective 3 is closer to the output sum of the adjacent load nodes. The trend proximity index are 0.4922, 0.5052, 0.4862 in turn. The benefits of the local scheduling layer corresponding to the control objective 3 will be further demonstrated in the subsequent scheduling result.

The voltage control methods of VSCs are divided into two cases, case 1: single-point voltage control mode, VSC 1: Constant U_{dc}, Q_s, VSC 2,3: Constant P_s, Q_s. Case 2: voltage-droop control mode, VSC 1, 2: $U_{dc} - P_{dc}$ voltage-droop, Constant Q_s, VSC 3: Constant P_s, Q_s.

The result of different energy storage control objectives with 0.95 confidence are given in Table 2. It can be seen that the energy storage control mode 3 has obvious advantages in reducing the total dispatching cost, the network losses and the

TABLE 2. Optimized results of 0.95 confidence under different energy storage control modes.

Case	Total dispatching cost/¥	Voltage deviation	Network losses/MW	Abandon wind power/MW	Abandon PV power/MW
Obj1-case1	50331	1366.0	14.434	6.6774	0.2912
Obj2-case1	50278	1279.7	14.2836	6.6115	0.2908
Obj3-case1	48171	1280.4	13.3613	2.5047	0.0293
Obj1-case2	49924	1256.3	12.9648	6.4283	0.4139
Obj2-case2	49977	1215.7	13.3475	6.9164	0.5150
Obj3-case2	47915	1202.1	11.6929	2.8681	0.1675

TABLE 3. Optimized results of different confidence levels under the energy storage control mode 3.

Case	Total dispatching cost/¥	Voltage deviation	Network losses/MW	Abandon wind power/MW	Abandon PV power/MW
0.95-case1	48171	1280.4	13.3613	2.5047	0.0293
0.90-case1	46904	1260.3	11.916	0.264	0.019
0.80-case1	45752	1346.1	11.1346	0.3139	0.00085
0-case1	45087	1309.4	9.6892	0.00014	0
0.95-case2	47915	1202.1	11.6929	2.8681	0.1675
0.90-case2	46688	1247.2	11.069	1.0881	0.071
0.80-case2	45437	1224.1	10.4494	0.5388	0.1105
0-case2	44854	1268.8	9.4752	0.4741	0.0639

amount of abandoned wind power and photovoltaic power. For example, Obj3-case1 has decreased by 4.3%, 7.4% and 63.6% respectively compared with Obj1-case1. The result of the voltage deviation index under three energy storage control modes are basically similar.

Table 3 gives the optimization results of the energy storage control mode 3 under different confidence levels. It can be seen that the total dispatching cost, network losses and abandoned wind power and photovoltaic power decreases with the decrease of confidence, which accords with the fact that the flexibility resources that the system needs reduce when the flexibility demand decreases gradually. In this paper, part of RES output (10% real-time wind power output maximum and 20% photovoltaic real-time output maximum) is considered in the flexible resource dispatching. As the demand for flexibility increases, the amount of wind and PV abandonment increases gradually. In addition, the voltage deviation is basically independent of the change of confidence.

Fig. 11 shows the system network losses corresponding to different confidence levels under the energy storage control mode 3. With the increase of confidence, the network losses increase gradually. The network losses under the voltage-droop control mode is lower than that under single-point voltage control mode. The operation losses of VSCs are much smaller than that under single-point voltage control mode. The reason is that VSC 1 and VSC 2 are selected as two voltage stations under the voltage-droop control. They undertake the tasks of power distribution and voltage adjustment together which effectively improves the operation parameters of VSCs. The decrease of I_{ci} leads to the reduction of the losses of VSC $P_{closs i}$.

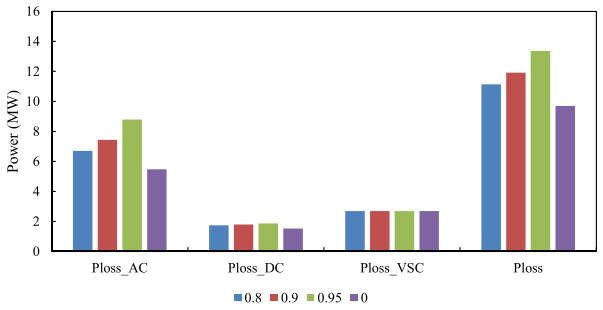

(a) Network losses of Obj3-case1 of different confidence degrees

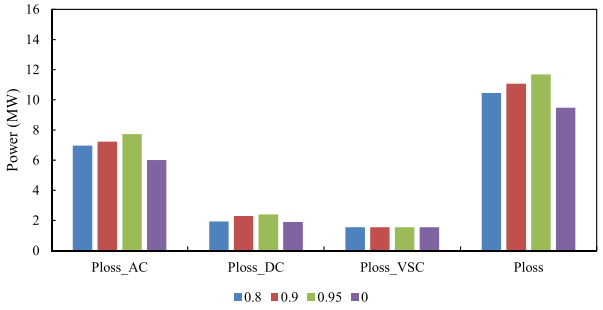

(b) Network losses of Obj3-case2 of different confidence degrees

FIGURE 11. Network losses of different confidence degrees under the energy storage control mode 3.

Figure. 12 shows the node voltages at 12:00 (AC node 1-33, DC node 34-39) under different confidences and voltage control modes of the energy storage mode 3 respectively. It can be seen that the influence of confidence on the node voltages at a single time is small under the framework of the model, but the node voltage level is highest when the flexibility

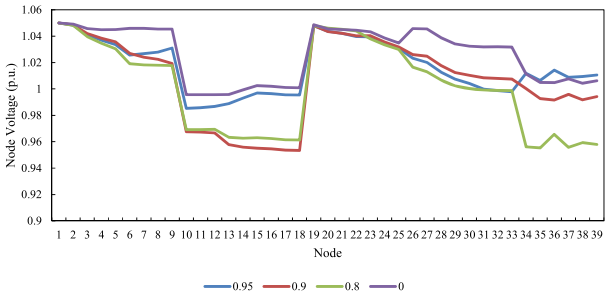

(a) Node Voltages at 12:00 of Obj3-case1

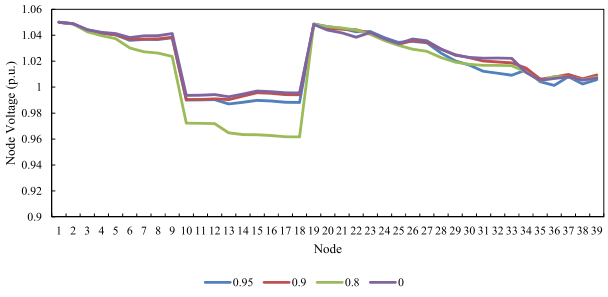

(b) Node Voltages at 12:00 of Obj3-case2

FIGURE 12. Node Voltages at 12:00 under the energy storage control mode 3.

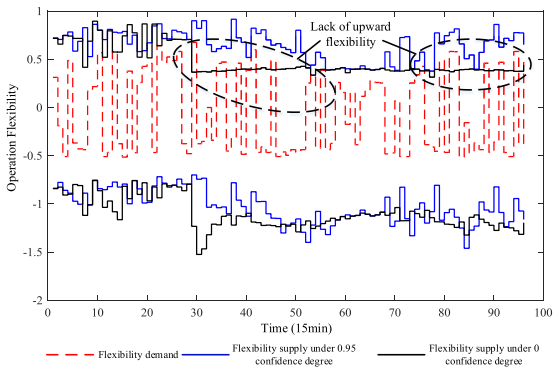

(a) Analysis of system flexibility of single-point voltage control under the energy storage control mode 3

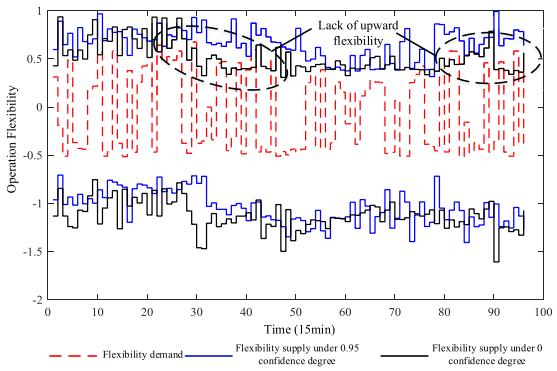

(b) Analysis of system flexibility of voltage-droop control under the energy storage control mode 3

FIGURE 13. Analysis of system flexibility under the energy storage control mode 3.

requirement constraint is not taken into account. Compared with the single-point voltage control mode, the node voltage changes more smoothly and the voltage level is higher under the voltage-droop control mode. The voltage control mode of VSCs will directly affect the node voltage level of the flexible operation.

TABLE 4. Load parameters of modified IEEE-33 system.

Node	P (MW)	Q (Mvar)	Node	P (MW)	Q (Mvar)
1	0	0	18	0.09	0.04
2	0.1	0.06	19	0.09	0.04
3	0.09	0.04	20	0.09	0.04
4	0.12	0.08	21	0.09	0.04
5	0.06	0.03	22	0.25	0.15
6	0.06	0.02	23	0.09	0.05
7	0.2	0.1	24	0.1	0.06
8	0.2	0.1	25	0.35	0.25
9	0.06	0.02	26	0.06	0.025
10	0.06	0.02	27	0.06	0.025
11	0.045	0.03	28	0.06	0.02
12	0.06	0.035	29	0.12	0.07
13	0.2	0.1	30	0.1	0.06
14	0.12	0.08	31	0.06	0.02
15	0.06	0.01	32	0.08	0.03
16	0.06	0.02	33	0.42	0.2
17	0.06	0.02	-	-	-

Note: The node 22, 25 and 33 are industrial loads. The node 4, 13 and 29 are office loads. The rest are residential loads.

Fig. 13 shows the flexible supply of dispatching results and the flexible demand for the actual operation under the confidence of 0.95 and 0 for the energy storage control mode 3. Considering the flexible supply and demand of single-point voltage control and voltage-droop control, it can be seen that the dispatching results without considering the flexible demand are not flexible enough in some time of actual operation, but flexible enough in downward supply. It is closely related to the characteristics of the right deviation of the actual wind power error distribution. Comparing the dispatching results under 0.95 confidence, the system can always cope with the uncertain fluctuation in the actual operation process without causing insufficient climbing and load shedding. It can be seen that under the premise of taking into account the uncertainty of wind power, fully dispatching the uncertain resources can effectively enhance the system's ability to cope with uncertain fluctuations, further improve the permeability of RES and ensure a safe, stable and flexible operation of distribution networks under high permeability.

TABLE 5. Operating parameters of energy storage systems.

No	Minimum of charging and discharging power (MW)	Maximum of charging and discharging power (MW)	Minimum state of charge	Maximum state of charge
1	0	0.15	0.2	0.9
2	0	0.15	0.2	0.9
3	0	0.12	0.2	0.9
No	Maximum capacity (MW*h)	Initial capacity (MW*h)	Consumption rate	Charging and discharging ratio
1	0.8	0.3	0.001	0.9
2	0.8	0.3	0.001	0.9
3	0.6	0.25	0.001	0.9

TABLE 6. Load parameters of the DC network (distribution coefficients).

Node	Type	Distribution coefficients
1	1	0
2	1	0
3	1	0
4	2	0.08
5	1	0.05
6	1	0.07

Note: The node type 1 is office loads and type 2 is the electric vehicle load.

TABLE 7. Operation parameters of AC side, loss characteristics and capacities of three-terminal MTDC.

VSC	Transformer Z_t (p.u.)	Filter B_f (p.u.)	Commutation reactance Z_c (p.u.)	Loss characteristics a, b, c/10^{-3}	Capacity S (p.u.)
1	0.001+j0.033	0	0.05	0.8, 1.1, 1.5	0.24
2	0.0015+j0.05	0	0.15	0.45, 1.2, 1.1	0.12
3	0.003+j0.1	0.1	0.15	0.9, 1, 1.5	0.12

TABLE 8. Parameters of DC lines and nodes.

Node i	Node j	Line resistance (p.u.)	Power of Node j (kW)	Load of Node j (kW)
1	4	0.125	0	300
2	4	0.09		
2	5	0.095	150	400
3	5	0.12		
1	6	0.1	200	450
3	6	0.13		

TABLE 9. Time-of-use electricity price.

Category	Concrete time	Price（¥/kW·h）
Peak period	11：00-15：00、18：00-21：00	0.89
Normal period	07：00-11：00、15：00-18：00、21：00-00：00	0.49
Valley period	00：00-07：00	0.25

TABLE 10. Operation and maintenance costs of all kinds of devices in distribution network.

No	Parameter	Unit	value
1	c_{wt}	¥/kW·h	0.065
2	c_{pv}	¥/kW·h	0.055
3	c_{ess}	¥/kW·h	0.05
4	c_{fl}	¥/kW·h	1.5
5	c_{mt}	¥/kW·h	0.35
6	c_{ev}	¥/kW·h	0.02
7	c_{wp}	¥/kW·h	0.2
8	c_{pp}	¥/kW·h	0.2

VI. CONCLUSION

Based on the analysis of flexible supply and demand balance of AC/DC distribution networks with high-permeability RES, the paper quantitatively evaluates the source-network-load factors from the perspective of the operation flexibility and proposes the operation flexibility index and its calculation method. By using the kernel density estimation method and confidence interval method, the flexibility requirement constraints considering the uncertainty of the wind power are transformed and applied to the day-ahead flexible economic dispatching model. The following conclusions are drawn from the simulation:

(1) The operation flexibility index of AC/DC distribution networks embodies directionality, state dependence and multi-temporal-space characteristics. The flexible adjustable range of controllable flexibility resources under operational constraints is taken into account in the calculation method. It is suitable for the optimal dispatching of AC/DC distribution networks with high-permeability RES.

(2) The flexible demand constraints transformation method can realize the flexible demand transformation and characterization of the uncertainty of wind power, which makes the dispatching results both economical and flexible.

(3) The multi-objective flexible economic dispatching model which takes the uncertainty of wind power into account, can cope with the uncertain fluctuation while ensuring the flexible operation. It further reduces the network

losses, improves the node voltage level, better accepts RES and reduces the total dispatching cost.

APPENDIX

See Tables 4–10.

REFERENCES

[1] T. Mai, R. Wiser, D. Sandor, G. Brinkman, G. Heath, P. Denholm, D. J. Hostick, N. Darghouth, A. Schlosser, and K. Strzepek, "Exploration of high-penetration renewable electricity futures: Renewable electricity future study," Nat. Renew. Energy Lab., Golden, CO, USA, Tech. Rep., 2012, vol. 1.

[2] G. Schellekens, A. Battaglini, J. Lilliestam, J. McDonnell, and A. Patt, *100% Renewable Electricity: A Roadmap to 2050 for Europe and North Africa*. London, U.K.: PricewaterhouseCoopers, 2010.

[3] C.-S. Wang and P. Li, "Development and challenges of distributed generation, the micro-grid and smart distribution system," *Autom. Electr. Power Syst.*, vol. 34, no. 2, pp. 10–14, Jan. 2010.

[4] C. Wang and P. Li, "A review of CIRED 2011 on development of distributed energy resources and energy efficiency improvement on customer side," *Autom. Electr. Power Syst.*, vol. 36, no. 2, pp. 1–5, Jan. 2012.

[5] O. Samuelsson, S. Repo, R. Jessler, J. Aho, M. Kärenlampi, and A. Malmquist, "Active distribution network—Demonstration project ADINE," in *Proc. IEEE PES Innov. Smart Grid Technol. Conf. Eur.*, Gothenburg, Sweden, Oct. 2010, pp. 1–8.

[6] X. Chen, K. Chen, J. Liu, X. Ding, and K. Yu, "A distribution network intelligent dispatching mode and its key technique," *Autom. Electr. Power Syst.*, vol. 36, no. 18, pp. 22–26, Sep. 2012.

[7] F. Pilo, G. Pisano, and G. G. Soma, "Advanced DMS to manage active distribution networks," in *Proc. IEEE Bucharest PowerTech Conf.*, Bucharest, Romania, Jun./Jul. 2009, pp. 1–8.

[8] M. J. Dolan, E. M. Davidson, I. Kockar, G. W. Ault, and S. D. J. McArthur, "Distribution power flow management utilizing an online optimal power flow technique," *IEEE Trans. Power Syst.*, vol. 27, no. 2, pp. 790–799, May 2012.

[9] *Potential Reliability Impacts of Emerging Flexible Resources*, North Amer. Electr. Rel. Corp., Atlanta, Georgia, 2010, pp. 2–6.

[10] J. Adams, M. O'Malley, and K. Hanson, *Flexibility Requirements and Potential Metrics for Variable Generation: Implications for System Planning Studies*. Princeton, NJ, USA: NERC, 2010, pp. 14–17.

[11] H. Chandler, *Empowering Variable Renewables—Options for Flexible Electricity Systems*. Paris, France: International Energy Agency, 2008.

[12] Z. Lu, H. Li, and Y. Qiao, "Flexibility evaluation and supply/demand balance principle of power system with high-penetration renewable electricity," *Proc. CSEE*, vol. 37, no. 1, pp. 9–20, Jan. 2017.

[13] W. Liu, H. Li, H. Zhang, and Y. Xiao, "Expansion planning of transmission grid based on coordination of flexible power supply and demand," *Autom. Electr. Power Syst.*, vol. 42, no. 5, pp. 56–63, Mar. 2018.

[14] P. T. Baboli, S. Bahramara, M. P. Moghaddam, and M.-R. Haghifam, "A mixed-integer linear model for optimal operation of hybrid AC-DC microgrid considering renewable energy resources and PHEVs," in *Proc. IEEE Eindhoven PowerTech*, Eindhoven, The Netherlands, Jun./Jul. 2015, pp. 1–5.

[15] C. Qi, K. Wang, Y. Fu, G. Li, B. Han, R. Huang, and T. Pu, "A decentralized optimal operation of AC/DC hybrid distribution grids," *IEEE Trans. Smart Grid*, vol. 9, no. 6, pp. 6095–6105, Nov. 2018.

[16] X. Ma, R. Guo, L. Wang, J. Huang, J. Liu, and C. Fang, "Day-ahead scheduling model for AC/DC active distribution network based on second-order cone programming," *Autom. Electr. Power Syst.*, vol. 42, no. 22, pp. 144–153, Nov. 2018.

[17] L. Dong, T. Meng, N. Chen, Y. Li, and T. Pu, "Optimized scheduling of AC/DC hybrid active distribution network using Markov chains and multiple scenarios technique," *Autom. Electr. Power Syst.*, vol. 42, no. 5, pp. 147–153, Mar. 2018.

[18] G. Zhou, M. Zhou, L. Sun, Z. Guo, J. Gu, and Y. Sun, "Research on operational flexibility evaluation approach of power system with variable sources," *Power Syst. Technol.*, vol. 43, no. 6, pp. 2139–2146, Jun. 2019.

[19] H. Wang, S. Wang, Z. Pan, and J. Wang, "Optimized dispatching method for flexibility improvement of distribution network with high-penetration distribution generation," *Autom. Electr. Power Syst.*, vol. 42, no. 15, pp. 86–93, Aug. 2018.

[20] Q. Wang and B.-M. Hodge, "Enhancing power system operational flexibility with flexible ramping products: A review," *IEEE Trans. Ind. Inf.*, vol. 13, no. 4, pp. 1652–1664, Aug. 2017.

[21] S. Liu, M. Miao, T. Shi, and J. Li, "Optimal power flow in hybrid AC/DC distribution network considering different control strategies of VSC stations," in *Proc. IEEE China Int. Conf. Electr. Distrib. (CICED)*, Sep. 2018, pp. 1380–1384.

[22] M. Cui, J. Zhang, Q. Wang, V. Krishnan, and B.-M. Hodge, "A data-driven methodology for probabilistic wind power ramp forecasting," *IEEE Trans. Smart Grid*, vol. 10, no. 2, pp. 1326–1338, Mar. 2019.

[23] X.-Y. Ma, Y.-Z. Sun, and H.-L. Fang, "Scenario generation of wind power based on statistical uncertainty and variability," *IEEE Trans. Sustain. Energy*, vol. 4, no. 4, pp. 894–904, Oct. 2013.

[24] X. J. Liu and C. Y. Xie, "Wind power fluctuation interval estimation based on beta distribution," *Electr. Power Autom. Equip.*, vol. 34, no. 12, pp. 26–30, Dec. 2014.

SHAN GAO (M'07) received the Ph.D. degree from Southeast University, Nanjing, China, in 2000, where he is currently an Associate Professor with the School of Electrical Engineering and the Jiangsu Provincial Key Laboratory of Smart Grid Technology and Equipment. His research interests include power system planning and operation, renewable energy integration, and active distribution networks.

SAI LIU was born in Suqian, China, in 1993. He received the B.S. and M.S. degrees in electrical engineering from the School of Electrical Engineering, Southeast University, Nanjing, China, in 2016 and 2019, respectively. He is currently with State Grid Jiangsu Electric Power Company Ltd., Maintenance Branch Company. His current research interests include the optimization and operation of the hybrid ac/dc distribution networks.

YU LIU (S'15–M'19) received the B.S., M.S., and Ph.D. degrees in electrical engineering from the School of Electrical Engineering, Southeast University, Nanjing, China, in 2011, 2014, and 2018, respectively. From 2015 to 2016, he was a Visiting Scholar with the University of Alberta, Edmonton, Canada. He is currently a Lecturer with the School of Electrical Engineering, Southeast University, and the Jiangsu Provincial Key Laboratory of Smart Grid Technology and Equipment. His research interests include power system planning and operation, integrated energy systems, and non-intrusive load monitoring.

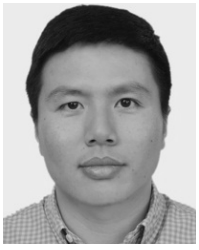

XIN ZHAO received the B.S., M.S., and Ph.D. degrees in electrical engineering from the School of Electrical Engineering, Southeast University, Nanjing, China, in 2005, 2008, and 2014, respectively, where he is currently a Lecturer with the School of Electrical Engineering. His research interests include sub-synchronous oscillation, and power system stability control and planning.

TIANCHENG E. SONG received the B.S. degree in agribusiness from the University of Saskatchewan, Saskatoon, SK, Canada, in 2012, and the M.Eng. degree in electrical engineering from Southeast University, Nanjing, China, in 2019. He is currently pursuing the Ph.D. degree in electrical engineering with Southeast University. From 2012 to 2016, he worked in the fields of grain and lumber trading at Cargill Ltd. and Mitsui & Company Ltd. His research interests include power market, steady state analysis, and grain market risk management.